Impact of phase change materials and brick thickness on thermal comfort in free-floating mode

D. Abd El-Raheim[1, *], A. Mohamed[1], M. Fatouh[1], H. Abou-Ziyan[1]

[1] Department of Mechanical Power Engineering, Faculty of Engineering at El-Mataria, Helwan University, Massaken El-Helmia, P.O. 11718, Cairo, Egypt.

1 Abstract

In this paper, a simulation model is developed to predict the effects of phase change materials (PCMs) with different perforated brick thicknesses on the thermal comfort of heavy structural buildings in a free-floating mode under the hot-dry conditions. According to Egyptian building standards, a room with a floor area of 16m² and a height of 3m is simulated under Cairo (Egypt) weather conditions. Two PCMs with melting temperatures of 29 and 25°C and perforated brick thicknesses of 10, 15, 20, 25, and 30 cm are used and evaluated in terms of the exceeding hours, the time lag, and the decrement factor. The simulation model is validated using data reported in the literature for an outdoor cubicle. The results confirmed that the installed PCM layer into the building envelope saves the building's usable area and reduces the initial cost of construction. When the PCM-29 layer is integrated with a 20 cm thick perforated brick, the maximum exceedance hours are reduced by nearly 620 hours compared to 10 cm brick thickness. Combining the PCM layer with the 10 cm thick perforated brick achieved the same exceeding (approximately 1383) hours as the 20 cm thick base case. Seasonal assessment of PCMs revealed that the best PCM behavior varies according to outdoor temperature fluctuations. PCM-25 produces better indoor operative temperature than PCM-29 in spring and vice versa in summer. As the perforated brick thickness increased from 10 cm to 30 cm, the charging time required to melt 5% PCM-25 increased from 3.5 hours to 22 hours. In addition, when the brick thickness is 15 cm, the maximum time lag difference of the PCM-25 layer is about 7.25h. In summer, PCM is most effective when the thickness of the perforated bricks is 20 cm.

Keywords: Building envelope, phase change material, free-floating mode, exceeding hours, liquid fraction, and time lag.

***Corresponding Author** **diaa_mohammed@m-eng.helwan.edu.eg**

Nomenclature

DF	Decrement factor (-)
EH	Exceeding hours (h.)
R	thermal resistance (m^2K/W)
T	temperature (^oC)
TL	Time lag (h)
U	overall heat transfer coefficient (W/m^2K)
C	the space discretization constant (-)
c_p	specific heat (J/kgK)
f	Liquid fraction (-)
h	enthalpy (kJ/kg)
k	thermal conductivity (W/m K)

Greek symbols

α	thermal diffusivity (m^2/s)
$\Delta\tau$	time interval (sec) or discomfort time (h)
Δx	space step (m)
ρ	density (kg/m^3)

Subscripts

iop	indoor operative
m	melting
si	indoor surface

Acronyms

BSP	building simulation program
PCM	phase change material
PCM-T	phase change material categorized by its melting temperature

2 INTRODUCTION

The building envelope plays a main role in controlling the building energy consumption by adjusting the heat exchange between the indoor and outdoor environments to satisfy the building's thermal requirements [1]. A recent report from the International Energy Agency (IEA) states that most of the investment and spending in the building sector is in the renovation and construction of building envelopes [2]. This report further revealed that building construction and operations accounted for 36% of the final global energy used in buildings and 39% of the energy-related CO_2 emissions. Current construction codes encourage and stress the reduction of energy consumption in buildings [2]. One of these needs is the traditional approach of using a high resistance building envelope, by adding insulation or increasing wall thickness. Alternative strategies rely on improving the thermal energy storage of the building envelope to enhance the dynamic behavior of the wall thermal capacity [3]. When using phase change material (PCM) in a building envelope; as outside air temperature increases during the daytime, PCM absorbs large amounts of heat and changes its phase from solid to two-phase and then liquid. Thus in the two-phase region, the heat is stored in the form of latent thermal energy. This two-phase process can be accomplished within a limited temperature range (phase change temperature).

During the nighttime, as the outside temperature decreases, the thermal energy stored can be discharged automatically to the outside PCM layer, with the PCM changing status from liquid to solid, this heat is released and solidification occurs to the PCM when the PCM temperatures drop below the onset of the PCM solidification [4,5].

Numerous experimental works were carried out on small models to investigate the benefits of PCMs integrated into buildings in the free-floating mode under different weather conditions. In the free-floating mode, the building's interior temperature fluctuates freely without any mechanical cooling. Castell et al. [6] experimentally investigated the effect of using a PCM panel with a melting temperature of 27°C in a room and compared it with a traditional room in Spain. The results showed that PCM can reduce peak temperature by 1°C and delay it by 6hours. Silva et al. [7] experimentally observed that the swing temperature decreased from 10°C in the reference chamber to 5°C with an increase in the time lag of 3 h when using PCM with a melting temperature of 18°C. Also, Athienitis et al. [8] experimentally and numerically evaluated the performance of PCM combined with gypsum wallboard in a room located in Montreal. They showed that the maximum room temperature during the day was 4°C lower.

The time lag (TL) and decrement factor (DF) are important parameters, which can be used to analyze the dynamic characteristics of conventional walls with different thicknesses and building materials. Evaluation of these parameters provides a way to improve the thermal comfort level [9]. The effect of wall thickness on TL and DF is discussed in several publications. Thongtha et al. [10] reported that the time lag is directly proportional to the wall thickness, while the decrement factor is inversely proportional to the wall thickness. Bilgin and Arici [11] found through a simulation model that for the PCM wall in Ankara, Turkey, TL increased from 5.64 to 16.11h, and DF decreased from 0.144 to 0.034. Kuznik et al. [12] concluded that the PCM layer increases the TL by 1.66 hours. Kong et al. [13] found that the room with the PCM layer on the inside was 2°C cooler than the reference room, and the maximum temperature inside the wall was delayed by about 3 hours.

The above literature review revealed that PCM integrated into buildings is one of the promising passive cooling technologies. Various researchers have evaluated the thermal performance potential of PCMs on indicators of indoor thermal comfort in buildings. However, a few studies have focused on the effect of integrated PCMs with different building envelope thicknesses on thermal comfort. The thermal performance of PCMs with different wall thicknesses, including heavyweight structures, has not been fully explored under hot climatic conditions [14,15].

The present work investigates the effect of brick thickness and type of PCM on thermal comfort in the building during a free-floating mode based on the exceeding hours. The effect of the PCM layer and wall thickness was evaluated by TL, DF, and PCM efficacy. Furthermore, the current study aimed to compare different wall thicknesses with and without PCM to explore the benefits of the presence of PCM on the indoor thermal comfort of buildings. To achieve the goals of the present work, a room with different brick thicknesses integrated with two different

PCMs with melting temperatures of 25°C and 29°C is tested under the hot climate of Cairo using the Design-Builder and EnergyPlus as simulation tools.

3 Material and Methods

3.1 Case Study

A testing room with various envelopes (composite wall and roof) is simulated. Conventional brick without PCM and with different types of PCM layers are integrated into the external walls and roof. The detailed construction of the different room elements is presented in Table 1. The floor area of the room is 16 m^2 (4m×4m) with 3m in height. The specifications of walls, roof, and window are selected according to Egyptian building standards [16,17].

Table 1 Thermophysical properties of the testing room

Material	Thickness (cm)	Density (kg/m^3)	Thermal conductivity (W/m.K)	Specific heat (J/kg.K)	Thermal resistance (m^2.K/W)
External wall:					
Cement mortar (outer)	2.7	1600	0.79	840	
Perforated brick	20	1790	0.6	840	0.555 (Base case)
PCM layer (in PCM model)	2.0	860	0.2	1970	0.655 (PCM case)
Plastering (inner)	1.0	1150	0.57	1000	
Roof:					
Tiles	2.0	2000	1.3	840	
Gravel	3.0	1840	0.36	840	
Water-proof membrane	0.5	35	0.034	1300	
Roof screed	5.0	1200	0.41	840	0.668 (Base case)
Reinforced concrete	5.0	2150	1.4	1000	0.768 (PCM case)
PCM layer (in PCM model)	20	860	0.2	1970	
Plastering	1.0	1150	0.57	1000	

All walls and the roof are exposed to the outdoor environment (the four-cardinal directions), except the floor which is in contact with the ground. The room has a window and door on the north facade. The area of the window and door are 0.7 and 1.8 m^2, respectively. The window is clear double glazing (each layer is 6 mm thickness) filled with a 6 mm air gap, the U_w=3.094 W/m^2K, and the shading coefficient is 0.75. The room is occupied by one person with a metabolic rate of 90W and air ventilation of 0.5 air change per hour based on air leakage through cracks. Other internal heat gains are about 40W and are kept constant in all simulation cases. It may be noted that a similar technique was reported by Castanzo et al. [18].

3.2 Numerical methods

The tested room is modeled using Design-Builder [19] and simulated with the EnergyPlus engine [20] to predict the thermal behavior of the room. For PCM, the Conductive Finite Difference (CondFD) algorithm combined with the enthalpy-temperature function (the enthalpy curve) is used to model its construction elements. The enthalpy-temperature function is used to develop the equivalent specific heat

$\left(c_{p,eq}^{n}\right)$ at each time step, as shown in Eq. (1). It is necessary to correctly define this curve in EnergyPlus to give a good prediction of PCM behavior [21].

$$c_{p,eq}^{n} = \frac{h^{n+1} - h^{n}}{T^{n+1} - T^{n}} \quad (1)$$

The liquid fraction of the PCM (f_{PCM}) in any case can be calculated by averaging the stored latent heat of all nodes, as shown in Eq. (2).

$$f_{\mathrm{PCM,eq}} = \sum_{0}^{j} \frac{h^{n} - h^{i}}{\Delta h} \quad (2)$$

Where h^{n} and h^{i} are the latent storage of j node at certain time n and the latent storage at onset melting temperature, while Δh is the total latent storage between end set and onset melting temperatures. The $f_{\mathrm{PCM,eq}}$ provides information about the state of the PCM, when f=0, the PCM is solid, and if f=1, the PCM is completely melted. Partially melted PCM can be identified as $0<f<1$ (two-phase region).

3.3 Input data

All simulations are run for a full year (8760 hours) using the standard weather file of Cairo, Egypt (representing a hot and dry climate), which is available on the EnergyPlus website [20]. The PCMs chosen are organic materials based on fatty acids and paraffin. The general thermophysical properties of the tested PCMs, under different melting ranges, are listed in Table 2. The tabulated input data of temperature-enthalpy pairs of the alternative PCMs provided by the manufacturers and supplied to the EnergyPlus are used to calculate the equivalent specific heat during the phase change process.

During the simulation of PCM with EnergyPlus [18,22,23], the following assumptions were considered; 1) the time step is equal to or less than 3 minutes, 2) the space discretization constant is 3, the relaxation factor is 1, 3) the heat transfer between the ground and the floor is calculated by the slab module. According to the EnergyPlus guideline [21], the PCM model is based on the following assumptions: 1) a continuous PCM layer with constant thickness, 2) PCM density is equal and constant in liquid and solid phases, 3) PCM thermal conductivity and specific heat are constant in each phase and may differ between solid and liquid phases, and 4) the effect of hysteresis, sub-cooling and phase segregation don't account during simulation.

Table 2 Thermophysical properties of the considered PCM [24,25]

Material	Peak melting temp., °C	Phase transition region, °C	Thermal conductivity in solid, W/m K	Specific heat in solid, J/kgK	Density in solid, kg/m^3	Heat of fusion, kJ/kg
PCM-25	25	23-27	0.2	1970	860	210
PCM-29	29	26-31	0.2	1970	860	210

4 Model validation and research program

4.1 Model validation

The accuracy and reliability of the proposed model are verified by experimental models in the literature [6,26]. The proposed model was compared with an actual test room in the free-floating mode in Puigverd de Lleida, Spain [6,26]. Two rooms were tested, one with a PCM layer and one without a PCM layer (as a reference room). In the reference cubicle, the walls consisted of cement mortar, hollow bricks, air chambers, perforated bricks, and plaster, while in the PCM cubicle, the same wall structure is used with 5 cm of polyurethane spray foam between the perforated brick and the air chamber. The roof composition in the two cubicles consists of concrete prefabricated beams, polyurethane material placed on the concrete with cement mortar, and a double bituminous membrane. The PCM layer (RT-27) is located between the perforated bricks and the polyurethane in the southern and western walls and the roof. The necessary input data related to RT-27 are selected and the enthalpy as a function of temperature is tabulated based on reference [6]. Both rooms are modeled using the same operating data that were used during the experimental week from the 2nd to the 7th of August [27]. The weather data files available on the Energy Plus website have been modified and the monthly weather data provided by Cabeza et al. [27] was used.

Figure (1) reveals the similarity between the experimental and predicted indoor air temperature for rooms with and without PCM. It can be observed that the match includes both peak and instantaneous values. Also, the peak indoor air temperature for the experimental and predicted cases is in the mid-afternoon between 10:00 pm to 12:00 am in each day. The average percentage errors are 2.8% and 1.5% for the cases without and with PCM, respectively. Therefore, the proposed model is accurate and able to predict the thermal behavior of buildings with and without PCM materials.

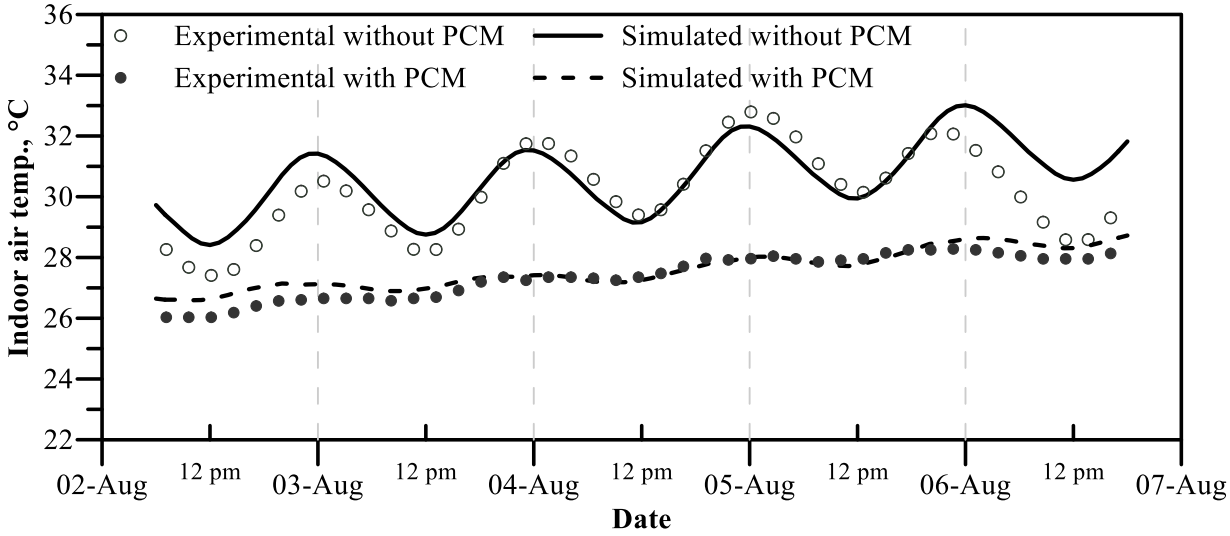

Figure 1 Experimental and simulated indoor air temperature for reference and PCM cubicles (2nd- 7th August)

4.2 Simulation procedure

This section presents a simulation procedure to evaluate the thermal behavior of the tested room with and without PCM in the free-floating mode under the climatic conditions of Cairo, Egypt, for the different seasons such as spring (16-18 May) and summer (2-8 July).

The present work is carried out in four steps. First, the effect of a brick thickness (10-30 cm) on indoor thermal comfort is predicted. Then, PCMs with melting temperatures of 25 and 29°C are evaluated and compared, and the performance metrics of walls with and without PCM layers are compared. In addition, the thermal performance of the PCM was estimated in all directions. Finally, the contribution of PCM layers to influencing seasonal indoor thermal comfort is explored.

Initially, the results are evaluated hourly to determine the behavior of the PCM in terms of indoor operating temperature, the number of exceeding hours (EH), time lag (TL), decrement factor (DF), and PCM liquid fraction (*f*). The indoor operative temperature (T_{iop}) is defined as the combined effect of convective and radiative heat transfer directly related to satisfaction. Exceeding hours (EH) is defined as the number of hours during a defined period during which the environmental conditions of the occupied space exceed the 90% acceptable limit of the adaptive comfort zone [28].

Despite large outdoor temperature fluctuations, time lag (TL) and decrement factor (DF) are important metrics to describe the relationship between the thermal storage capacity of building envelopes and indoor thermal comfort based on brick thickness. The calculation of the time lag of the exposed wall determines the time of the highest temperature on the surface of the inner and outer walls during this period. The period of the heat wave is a sinusoidal function and is considered to be the difference between the minimum values of the temperature distribution on the outer surface. The decrement factor is calculated based on the ratio between the maximum and minimum values of the indoor surface temperature and the maximum and minimum values of the outdoor surface temperature each day. It should be noted that the TL and DF for different directions are not equal. Therefore, the TL and DF of the room are calculated from the average of the four directions over a day. Additionally, these averages are calculated over two days that represent the climatic season.

The effectiveness of the PCM depends on the PCM hourly transient liquid fraction (*f*) in relation to the PCM temperature. Phase change materials are very efficient at $0<f<1$, i.e., in the two-phase region (activation). This fact means that it can store or release large amounts of latent heat. PCM does not store or release latent heat (non-activated) when the PCM fluid fraction (*f*) is zero (solid phase) or one (liquid phase). The PCM active time percentage is calculated over a given period during which the PCM undergoes a phase change that is directly related to the latent heat storage capacity of the PCM during the two-phase region.

5 Results and discussion

Figure 2 shows the hourly outdoor and indoor air temperatures of the test room during a specific period of the year (20th to 22nd June) in Cairo in the free-floating mode. This figure shows damping, swing temperature, and indoor operative temperature for two cases, the base case (without PCM) and the other case where a layer of PCM is added to the innermost layer of all exterior walls and roof. Damping is the reduction in peak zone operative temperature between the base case and the PCM case. The swing temperature is the difference between the maximum and the minimum temperatures throughout the day.

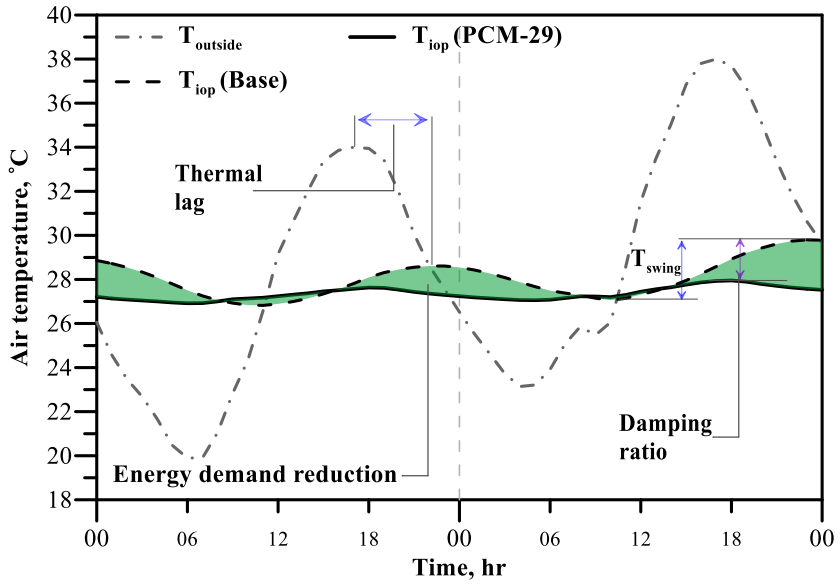

Figure 2 Air temperature change over time for two consecutive days in June

Clearly, the outdoor dry bulb temperature fluctuates between 38°C and 19.9°C, while the base case peak zone operative temperature of 29.8°C is reduced by 2.22°C when the PCM-29 layer is added. In addition, the average swing of T_{iop} is 2.74°C in the base case, which is in the shape of a sine wave curve, whereas using the PCM-29 layer causes a smaller average swing of about 0.9°C and an average indoor operative temperature of 27.45°C. Therefore, a more comfortable indoor environment can be obtained when PCM layers are used.

5.1 Effect of brick thickness

The effect of the brick thickness (10-30cm) on the indoor operative temperature can be predicted from Fig.3. In the base case, Fig. 3a shows that in spring, as the brick thickness increases from 10 to 30cm, the average peak T_{iop} decreases by about 3.73°C, while the mean minimum T_{iop} increases by about 1.54°C. This trend can be attributed to the increase in the heat capacity and thermal resistance, then the heat flow into the room is reduced. Consequently, the increased thermal resistance has a greater potential to reduce T_{iop}. In addition, thicker bricks help maintain a stable

and smooth distribution of the T_{iop} in the room. During summer, similar behavior for the base case is observed, as shown in Fig. 3b.

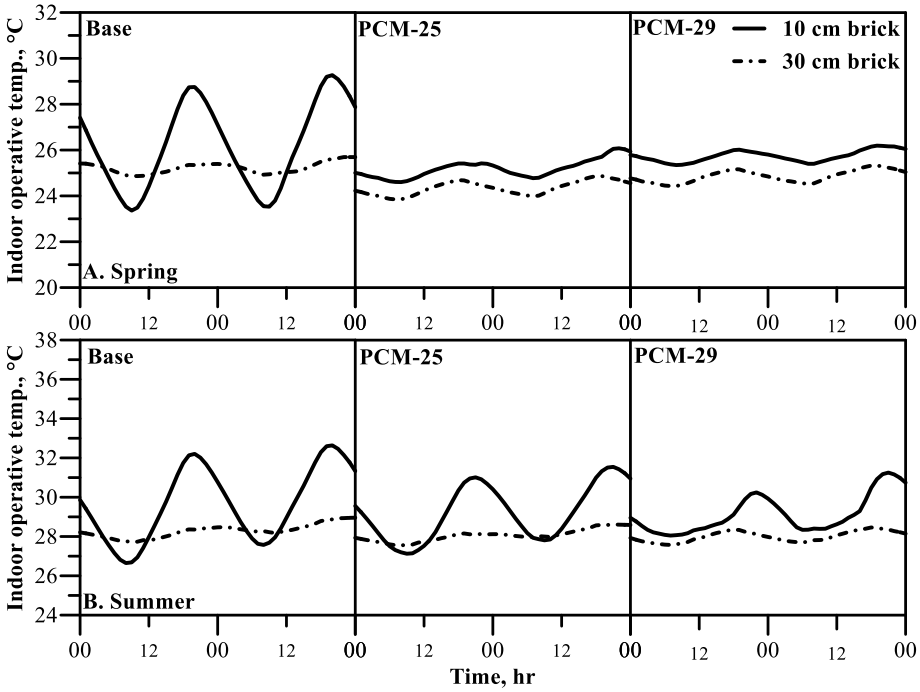

Figure 3 Effect of wall thickness and PCM layer on indoor operative temperature in different working conditions.

Figure 4 shows the average TL and DF for the different brick thicknesses that vary from 10 to 30cm during the spring and summer seasons. During the spring season, as the brick thickness increases from 10 to 30cm, the TL increases from 3.9 h to 11h (Fig.4a) whereas the value of DF decreases from 0.46 to 0.07 (Fig.4c). This fact is mainly due to the increase in the wall thermal resistance, which decreases the heat transfer across the wall. In addition, its heat storage capacity is enhanced. This means that the higher thermal resistance and heat capacity leads to an increase in the TL and a reduction in the DF. Similar trends and results were observed in summer, with the base case as shown in Fig. 4b and 4d.

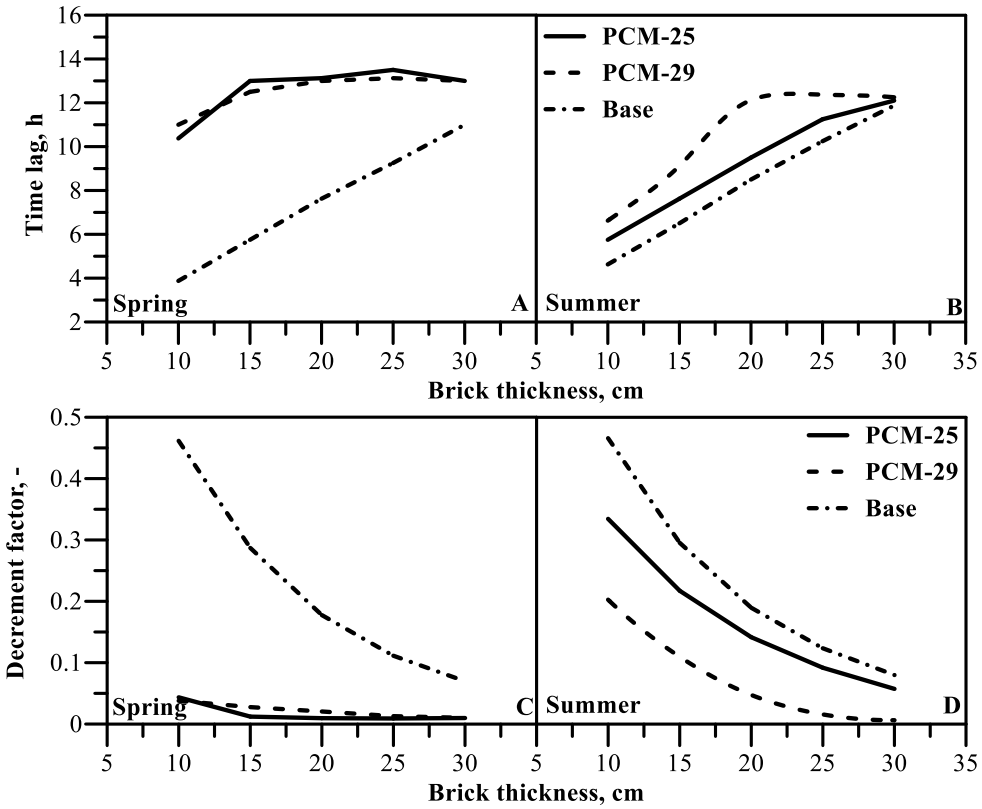

Figure 4 Effect of wall thickness on TL and DF in different working conditions

5.2 Effect of adding a PCM layer to different brick thicknesses

The effect of adding a PCM layer to different brick thicknesses (10 and 30 cm) on the indoor operative temperature and average liquid fraction, while other thermophysical properties remain unchanged, is shown in Figs. 3 and 5, respectively. Two PCMs with melting temperatures of 25 and 29°C were studied to predict indoor operative temperatures in the spring (Fig. 3a) and summer (Fig. 3b) seasons. All results were compared to a base case of 10 cm or 30 cm. The integration of the PCM layer with the brick has a more positive effect on indoor thermal comfort. In spring, as the brick thickness increases from 10 cm to 30 cm, the maximum damping in T_{iop} reduces from 3.5°C to 1°C for PCM-25 and from 3°C to 0.5°C for PCM-29, as shown in Fig.3a. This can be explained by the higher thermal resistance and heat capacity that causes the heat flow rate from the brick to the PCM layer to decrease, resulting in a lower temperature of the PCM layer.

Figure 4 reveals that integrating a PCM-25 or PCM-29 layer yields a longer TL and a lower DF than the base case for any brick thickness. Using PCM-25 layers in spring (Fig. 4b), the TL sharply increases, while DF decreases with increasing brick thickness from 10 cm to 15 cm. Then, the TL and DF remained almost unchanged when the thickness of the brick was increased from 15 cm to 30 cm. The average TL of PCM-25 is 2.26 and 2.28 times higher than that of the wall without PCM, while the average DF is reduced by 72% and 93% compared to the base case with brick thicknesses of 10cm and 15cm, respectively. Then, as the brick thickness is increased from 15 to 30 cm, the rate of increase in TL decreased compared to the base case.

This is because when the PCM-25 layer is combined with a brick thickness of 10cm, the state of the PCM is liquid most of the time. For a brick thickness of 15 cm, the maximum time lag difference between the PCM-25 layer and the base case is about 7.25 h.

The reason behind this trend in the time lag or DF is the decrease in thermal diffusivity and increase in heat capacity of the material. The thermal diffusivity of a wall with high thermal capacity is low and causes the TL value to increase and vice versa. However, lower thermal diffusivity results in a smaller DF for the room. When the brick thickness was increased to 30 cm, the PCM-25 layer was inactive most of the time and remained solid. This is because the heat transfer rate is lower for PCM layers integrated with large brick thickness compared to PCM layers with small brick thickness. This causes TL difference (between PCM-25 and base case) to decrease from 7.25h to 2h when the thickness of the brick increases from 15cm to 30cm. As shown in Fig. 4b, similar results were observed for the PCM-29 case.

During summer, the TL and DF trends for PCM-25 in Figs. 4b and 4d are like the base case. The TL is increased by 15% and the DF is decreased by 26% For the PCM-25 case compared to the base case. This is because PCM-25 remains liquid at high temperatures and acts as an insulating layer. With PCM-29, the time required for the melting process increases with brick thickness. This fact is due to a reduction in the rate of heat transfer to or from the PCM layer. The use of the PCM-29 layer results in a significant enhancement of TL, as shown in Fig. 4b. The average TL values of PCM-29 were increased by 15.2% and 27.6% while the DF was decreased by 40% and 66.4% compared to PCM-25 with brick thicknesses of 10 cm and 20 cm, respectively (Fig. 4d). This is due to the high latent heat of PCM-29 during the phase change. The PCM achieves the highest efficacy and TL when the thickness of the brick is 20 cm. Then, when the thickness of the bricks increased beyond 20 cm, the impact of the PCM decreased.

Furthermore, the average liquid fractions of the tested PCMs were investigated to evaluate the PCM performance, as shown in Fig. 5. As the thickness of the bricks increased from 10to 30cm, the mean f of PCM-25 decreased by 72% (Fig. 5a). In contrast, the PCM-29 layer remained solid (Fig. 5b) allowing more time for the two-phase operation. Fig. 5a shows that for a brick thickness of 10cm, the charging time to increase f_{PCM} from 0.55 to 0.6 is 3.5 h, while for a brick thickness of 30 cm, the charging time to increases f_{PCM} from 0.15 to 0.2 is 22 h over the first day during spring. This means that the charging time required to melt 5% of the PCM-25 with a brick of 30cm thick is much higher than with a brick of 10cm thick. In summer, the PCM-25 layer remains in the liquid state (f_{PCM} =1) and acts as an insulation layer under different brick thicknesses, while as the brick thickness increases from 10 to 30 cm, the average f_{PCM} reduces from 0.9 to 0.76 for PCM-29 (Fig.5b). The effect of PCM decreases as the brick thickness increases. This is because a thicker brick can reduce the PCM liquid fraction due to a reduction in heat exchange with the PCM layer. As a result, the melting time of the PCM is extended. Conversely, smaller brick thicknesses tend to accelerate the melting and solidification of the PCM process.

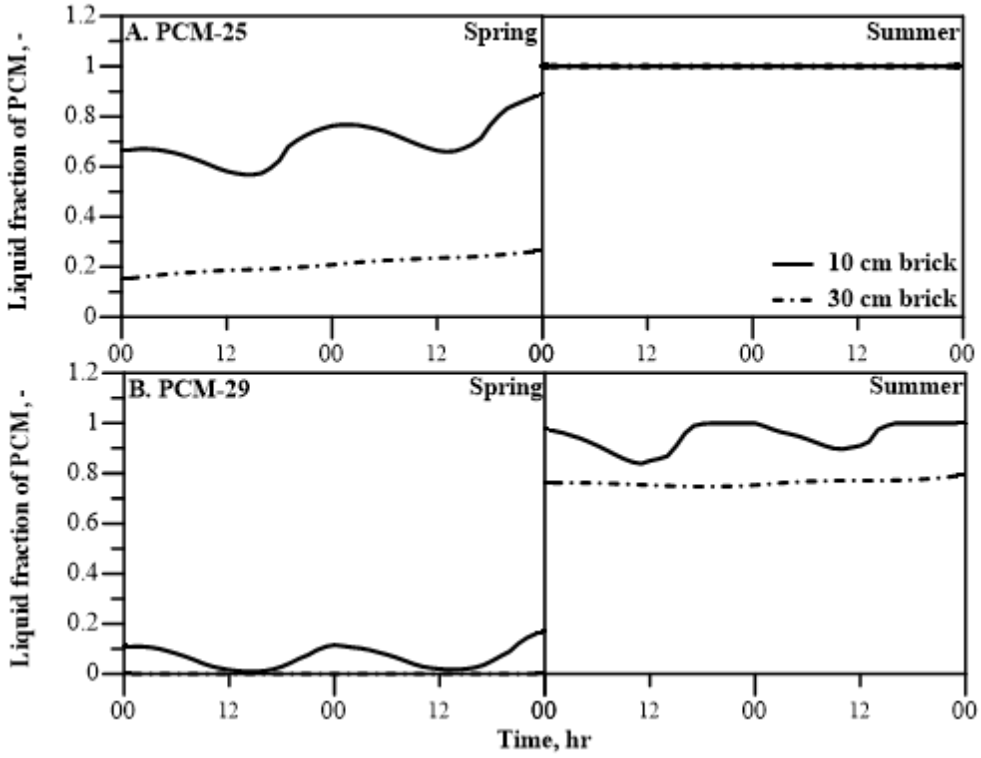

Figure 5 Effect of wall thickness on PCM liquid fraction in different working conditions

5.3 Effect of PCM layer orientation

The effect of PCM layer orientation on indoor surface temperature and PCM liquid fraction for two consecutive days in June is shown in Fig. 6. This figure compares the indoor surface temperature (T_{si}) in different directions for two cases (Base and PCM-29) during the same period. Clearly, the base case shows that the surface temperature varies between 26.5 and 31°C, depending on the air temperature and solar radiation. Furthermore, the difference between T_{si} in different directions is due to the different amounts of incident solar radiation in each direction. On the other hand, with the innermost surface PCM layer, the surface temperature does not seem to fluctuate and stabilizes at around 27.8°C. The reason behind that is due to the f_{PCM} values being between 0.35 and 0.8 in all directions (i.e., the PCM layer remains in a two-phase region). This means that the PCM layer that absorbs huge heat as latent heat during the daytime. This results in less heat flux through the enclosure and keeps the indoor operating temperature around 27.4°C.

During the daytime, the average values of f_{PCM} are around 0.67 and 0.755 on the first and second days, respectively. Thus, the PCM layer partially melts and turns into a liquid state. But during the night time in those days, the $T_{o,min}$ reduce to 19.9°C and 24.14°C, respectively. Hence, the PCM layer discharges the heat back to the indoor space. Consequently, the PCM layer was partially solid, and the average value of f_{PCM} on the first and second days are 49.3% and 53.4%, respectively.

It should be noted that the trends of transient f_{PCM} profile are different for the elements of the building envelope in the different directions as presented in Fig.6.

The swing in the f_{PCM} values of the north and south directions are high about (0.4°C) compared with (0.1°C) for the other directions. This is because the north and south walls receive lower solar radiation than the other vertical directions that receive higher solar radiation. It should be noted that the full thermal cycle (charging and discharging) of PCM cannot be completed in one day, this is not meaning the PCM is not perfectly working but reduces the potential of PCM. However, the nighttime ventilation strategies can improve the solidification process of PCM, which in turn provides higher latent heat storage for the next day during the day [29].

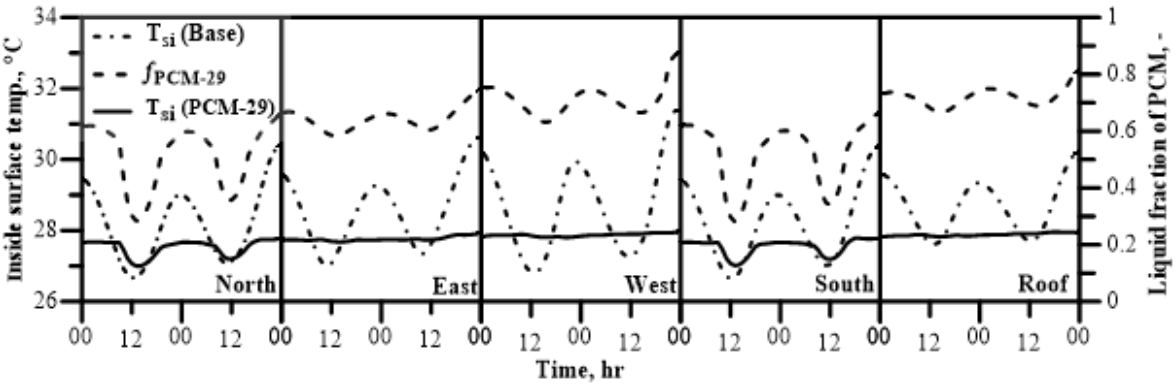

Figure 6 Changes in inside surface temperature and PCM liquid fraction for two consecutive days in June

5.4 Comparison between the investigated cases

Concerning the indoor thermal comfort during the long summer season from the start of April to the end of October, Fig.7 compares the exceeding hours for the tested brick thickness, which varies from 10 cm to 30 cm without and with PCM-25 or PCM-29. The exceeding hours assess the outcome of the PCM for the satisfaction of the indoor thermal environments. For the base case, as the brick thickness increases from 10 to 30cm, the exceeding hours decrease by 60%. This is due to the rise in total thermal resistance.

Figure 7 shows that the advantage of the presence of PCM in the room envelope over the base case is evident in EH reduction for different brick thicknesses. This is due to the increase in total thermal resistance and heat capacity during the phase change, as described in section 5.2. Table 3 shows that as the brick thickness increased from 10 to 30cm, the activation time of PCM-25 and PCM-29 decreased by 10.8% and 17.6%, respectively. This is because the heat transfer rate between the PCM layer and the brick decreases as the thermal resistance of the brick increases. Consequently, the PCM layer becomes inactive most of the time and remains in the solid-state. Hence, the PCM activation time diminishes, resulting in a reduction in the PCM efficacy, as well as a decrease in the EH reduction.

The use of the PCM-29 layer achieves the minimum exceeding hours compared to other cases at any brick thickness. Although the thermal resistance is equal in both PCM cases at each thickness, the difference in EH is due to the variation in the effective PCM activation time associated with the thermal storage rate for each PCM layer as observed in Table 3.

It can be observed that the PCM-29 layer integrated with the 20 cm brick achieved the maximum EH reduction of approximately (620 h) compared to that achieved by the other cases of brick thickness. This is because the PCM-29 has a maximum percentage active time of 49.57% and it stores the highest latent heat compared to the other cases.

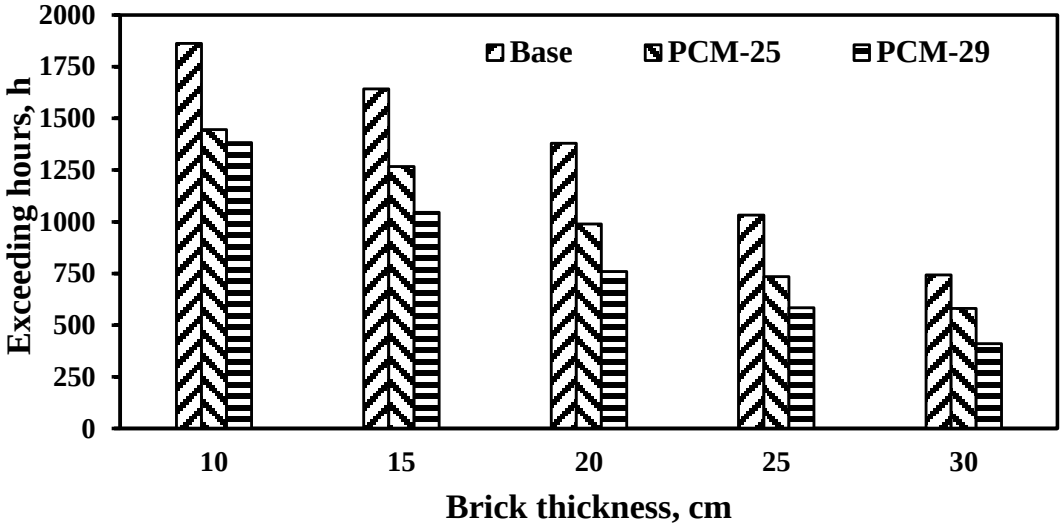

Figure 7 Effect of brick thickness combined with PCM layer on exceeding hours

Clearly, using PCM-25 or PCM-29 in combination with a small brick thickness (10 cm) provides better performance in the indoor thermal environment. For example, the thickness of the smallest brick (10cm) using PCM-29 produced an EH of 1383 h, which is comparable to the base case of 20cm thickness without the PCM layer. This means that the use of PCM can reduce the thickness of the wall while maintaining the same thermal comfort as thicker bricks. Consequently, increasing the building's usable area and, therefore, reduces the initial cost of construction.

Table 3 Seasonal PCM activation times for different brick thicknesses

Wall thickness, cm	PCM-25 activation time, %	PCM-29 activation time, %
10	42.5	67.9
15	39.4	64.9
20	38	62.2
25	38	58.8
30	37.9	56.0

6 Conclusions

In the present work, design-builder and EnergyPlus are used to develop a simulation model to investigate the effect of using two PCMs (PCM-25 and PCM-29) and various perforated brick thicknesses (10, 15, 20, 25, and 30cm) on the thermal comfort in a heavy-structure building. The simulation is carried out in a room

with a floor area of 16 m² and a height of 3m, built according to the Egyptian building standards in Cairo, Egypt, which represents dry-hot weather conditions. Based on the reported results, the following conclusions are drawn:

- Combining a thin PCM layer with a brick of 10cm thickness gives the same EH of 1383 hours as a 20cm thick brick.
- The PCM-29 layer integrated with 20cm bricks provided maximum EH reduction (approximately 620 hours) than the other cases of the same brick thickness during the investigated period.
- Seasonal assessment of PCMs showed that the best PCM varies according to outdoor temperature fluctuations. PCM-25 produces better performance than PCM-29 in spring and vice versa in summer.
- For the base case, the peak zone operative temperature was 29.8°C, which was reduced by 2.22°C with the addition of the PCM-29 layer.
- In spring, as the brick thickness increased from 10 to 30cm, the average liquid fraction is decreased by 72% for PCM-25 and from 0.9 to 0.76 for PCM-29.
- As the thickness of the brick is increased from 10to 30cm, the charging time required to melt 5% of PCM-25 increased from 3.5 hours to 22 hours.
- Using a PCM-25 or PCM-29 layer has a longer time lag and lower decrement factor than the base option for any brick thickness. In spring, when the thickness of the brick is 15 cm, the maximum time lag difference of the PCM-25 layer is about 7.25 hours. In summer, the PCM is most effective when the thickness of the bricks is 20 cm.
- The installed PCM layer into the building envelope saves the building's usable area and reducing in the initial cost of construction.

REFERENCES

[1] Q. Al-Yasiri, M. Szabó, Incorporation of phase change materials into building envelope for thermal comfort and energy saving: A comprehensive analysis, J. Build. Eng. 36 (2021). https://doi.org/10.1016/j.jobe.2020.102122.

[2] Key World Energy Statistics 2016, 2016. https://doi.org/10.1787/key_energ_stat-2016-en.

[3] A. Mavrigiannaki, E. Ampatzi, Latent heat storage in building elements: A systematic review on properties and contextual performance factors, Renew. Sustain. Energy Rev. (2016). https://doi.org/10.1016/j.rser.2016.01.115.

[4] D.A. Chwieduk, Dynamics of external wall structures with a PCM (phase change materials) in high latitude countries, Energy. (2013). https://doi.org/10.1016/j.energy.2013.06.066.

[5] X. Sun, M.A. Medina, Y. Zhang, Potential thermal enhancement of lightweight building walls derived from using Phase Change Materials (PCMs), Front. Energy Res. (2019). https://doi.org/10.3389/fenrg.2019.00013.

[6] A. Castell, I. Martorell, M. Medrano, G. Pérez, L.F. Cabeza, Experimental study of using PCM in brick constructive solutions for passive cooling, Energy

Build. (2010). https://doi.org/10.1016/j.enbuild.2009.10.022.

[7] T. Silva, R. Vicente, N. Soares, V. Ferreira, Experimental testing and numerical modelling of masonry wall solution with PCM incorporation: A passive construction solution, Energy Build. (2012). https://doi.org/10.1016/j.enbuild.2012.02.010.

[8] A.K. Athienitis, C. Liu, D. Hawes, D. Banu, D. Feldman, Investigation of the thermal performance of a passive solar test-room with wall latent heat storage, Build. Environ. (1997). https://doi.org/10.1016/S0360-1323(97)00009-7.

[9] R. Fathipour, A. Hadidi, Analytical solution for the study of time lag and decrement factor for building walls in climate of Iran, Energy. (2017). https://doi.org/10.1016/j.energy.2017.06.009.

[10] A. Thongtha, S. Maneewan, C. Punlek, Y. Ungkoon, Investigation of the compressive strength, time lags and decrement factors of AAC-lightweight concrete containing sugar sediment waste, Energy Build. 84 (2014). https://doi.org/10.1016/j.enbuild.2014.08.026.

[11] F. Bilgin, M. Arici, Effect of phase change materials on time lag, decrement factor and heat-saving, in: Acta Phys. Pol. A, 2017. https://doi.org/10.12693/APhysPolA.132.1102.

[12] F. Kuznik, J. Virgone, K. Johannes, In-situ study of thermal comfort enhancement in a renovated building equipped with phase change material wallboard, Renew. Energy. 36 (2011). https://doi.org/10.1016/j.renene.2010.11.008.

[13] X. Kong, S. Lu, J. Huang, Z. Cai, S. Wei, Experimental research on the use of phase change materials in perforated brick rooms for cooling storage, Energy Build. 62 (2013). https://doi.org/10.1016/j.enbuild.2013.03.048.

[14] Y. Cui, J. Xie, J. Liu, J. Wang, S. Chen, A review on phase change material application in building, Adv. Mech. Eng. (2017). https://doi.org/10.1177/1687814017700828.

[15] A. Baniassadi, D.J. Sailor, H.J. Bryan, Effectiveness of phase change materials for improving the resiliency of residential buildings to extreme thermal conditions, Sol. Energy. (2019). https://doi.org/10.1016/j.solener.2019.06.011.

[16] A. Visser, Florentine and Yeretzian, Energy Efficient Building: Guidelines for MENA Region, MED-ENEC Project Office, 2013.

[17] Energy Efficiency Building Code, Housing and Building National Research Center, Egypt, 2005.

[18] V. Costanzo, G. Evola, L. Marletta, F. Nocera, The effectiveness of phase change materials in relation to summer thermal comfort in air-conditioned office buildings, Build. Simul. (2018). https://doi.org/10.1007/s12273-018-0468-2.

[19] A. Tindale, DesignBuilder software, Des. Softw. Ltd. 6.1.3.008 (2019).

[20] U.S.D. of E. Doe, EnergyPlus Energy Simulation Software, Energyplus.

(2013).

[21] US Department of Energy, EnergyPlus Engineering Reference: The Reference to EnergyPlus Calculations, US Dep. Energy. (2010). https://doi.org/citeulike-article-id:10579266.

[22] M. Alam, H. Jamil, J. Sanjayan, J. Wilson, Energy saving potential of phase change materials in major Australian cities, Energy Build. (2014). https://doi.org/10.1016/j.enbuild.2014.04.027.

[23] P.C. Tabares-Velasco, C. Christensen, M. Bianchi, Verification and validation of EnergyPlus phase change material model for opaque wall assemblies, Build. Environ. (2012). https://doi.org/10.1016/j.buildenv.2012.02.019.

[24] Phase Change. Energy solutions, (2019). www.phasechange.com.

[25] RUBITHERM, Rubitherm® Technologies GmbH, (2019). https://www.rubitherm.eu/.

[26] J. Payá, J.M. Corberán, A. De Gracia, A. Castell, L.F. Cabeza, Thermal characterization of buildings from the monitoring of the AC system consumption, Energy Build. (2016). https://doi.org/10.1016/j.enbuild.2015.12.047.

[27] L.F. Cabeza, A. Castell, M. Medrano, I. Martorell, G. Pérez, I. Fernández, Experimental study on the performance of insulation materials in Mediterranean construction, Energy Build. (2010). https://doi.org/10.1016/j.enbuild.2009.10.033.

[28] ASHRAE, ANSI/ASHRAE Standard 55-2013, Ashrae Stand. (2013). https://doi.org/10.1007/s11926-011-0203-9.

[29] G. Evola, L. Marletta, F. Sicurella, A methodology for investigating the effectiveness of PCM wallboards for summer thermal comfort in buildings, Build. Environ. (2013). https://doi.org/10.1016/j.buildenv.2012.09.021.